34th Annual International Conference of the IEEE EMBS
San Diego, California USA, 28 August - 1 September, 2012

Automated Quantification of Atrial Fibrillation Complexity by Probabilistic Electrogram Analysis and Fibrillation Wave Reconstruction *

S. Zeemering, B. Maesen, J. Nijs, D. H. Lau, M. Granier, S. Verheule, and U. Schotten

Abstract—**The analysis of high-density activation maps of atrial fibrillation (AF) provides fundamental insights into the fibrillation wave propagation patterns and thus the mechanisms of AF. Current annotation of local activations in unipolar atrial electrograms and the construction of fibrillation waves require labor-intensive manual editing. To enhance the possibilities for spatiotemporal analysis of AF, we developed a rapid and fully automated procedure to accurately identify local, intrinsic atrial deflections and construct fibrillation waves based on these deflections. In this study, the automated procedure was validated using manually annotated electrograms and wave maps. We show that the novel procedure accurately detects intrinsic deflections (sensitivity=87%, positive predictive value=89%) and that reconstructed wave maps correlate well with manually edited wave maps in terms of number of waves (r=0.96), intra-wave conduction velocity (r=0.97), AF cycle length (r=0.97), and wave size (r=0.96) (p<0.01 in all cases). The automated procedure is therefore an adequate substitute for manual annotation.**

I. Introduction

Atrial fibrillation (AF) is an arrhythmia where the electrical activity in the atria is irregular instead of well organized. Multiple wavelets wander throughout the atria, instead of a single coordinated wave.[1] High-density atrial contact mapping of AF provides the most direct information on the spatiotemporal complexity of AF. It allows one to describe the process of AF in its most elementary form, the separate fibrillation waves.[2] From these wave propagation patterns it is possible to quantify the complexity of AF, for example in terms of the number of waves, the wave size, the wave conduction velocity or the wave source (peripheral or transmural breakthrough). Complexity of the AF activation pattern is a strong determinant of responsiveness to AF therapy. Assessment of the AF activation pattern might therefore be used for decision-making in the management of AF patients.[3] Current analysis methods still involve labor-intensive manual annotation of atrial deflections and waves, which limits the amount of fibrillation data that can be analyzed within a reasonable timeframe. Manual editing also increases the risk of subjective editing, which can lead to lower inter-observer consistency. To overcome these limitations we developed a novel method that identifies atrial deflections and fibrillation waves in a rapid and fully automated way, based on estimated probabilistic properties of the recorded fibrillation process. The details of this automatic procedure are presented in this paper, as well as the results of a validation study. In the design of the new deflection detection and wave mapping method, we aimed to incorporate electrophysiological knowledge to be able to compute wave map solutions that both visually and intellectually reflect the way electrophysiologists would construct them.

*This study was supported by a grant from the Dutch Research Organization (NWO, VIDI-grant 016.086.379), a grant from the Foundation Leducq (07CVD03), a grant from the Centre of Molecular Medicine (COHFAR), and a grant rom the European Union (FP7 Collaborative project EUTRAF, 261057).

S. Zeemering, D. H. Lau, M. Granier, S. Verheule and U. Schotten are appointed at the Department of Physiology, Maastricht University, P.O. Box 616, 6200 MD, Maastricht, The Netherlands (+31 (0)43 388 1320, e-mail: s.zeemering@maastrichtuniversity.nl).

B. Maesen and J. Nijs are appointed at the Department of Cardiothoracic Surgery, Maastricht University Hospital, Maastricht, The Netherlands.

II. Methods

A. Data acquisition

Unipolar atrial fibrillation electrograms were recorded in 15 patients during cardiac surgery using a 16x16 square grid of electrodes with an inter-electrode distance of 1.5mm. Acute AF was induced in 8 patients who were in sinus rhythm, 7 patients were already in AF during surgery (either paroxysmal or persistent AF). Signals were acquired from the epicardium of the right atrial free wall (RA) (n=15) and the posterior left atrium (LA) (n=11) with a sampling frequency of 1kHz. Segments of 4 seconds of AF were manually annotated by three experienced electrophysiologists to determine local atrial deflections and to identify clusters of deflections that form separate fibrillation waves, following the algorithm described in [2].

B. Electrogram pre-processing

The first step in processing the atrial measurements is to eliminate electrograms that exhibit a bad signal-to-noise ratio. To enable a valid comparison between the new method and manually annotated signals, the same electrograms were eliminated in both methods. Signals were then filtered with a third order zero-phase Chebyshev 0.5Hz high-pass filter to remove any baseline drift. Ventricular far-field disturbances in the atrial signal were removed by ventricular R-wave detection in a synchronously recorded ventricular signal [4], followed by single-beat QRST-template cancellation based on the adaptive singular value decomposition cancellation method by Alcaraz et al. [5]. This method determines the morphology of the QRST complex as the most significant principal component of a set of QRST windows in a single lead. We adapted this method to compute the QRST complex for a single *beat* in all electrograms to account for beat-to-beat QRST complex variability. In atrial

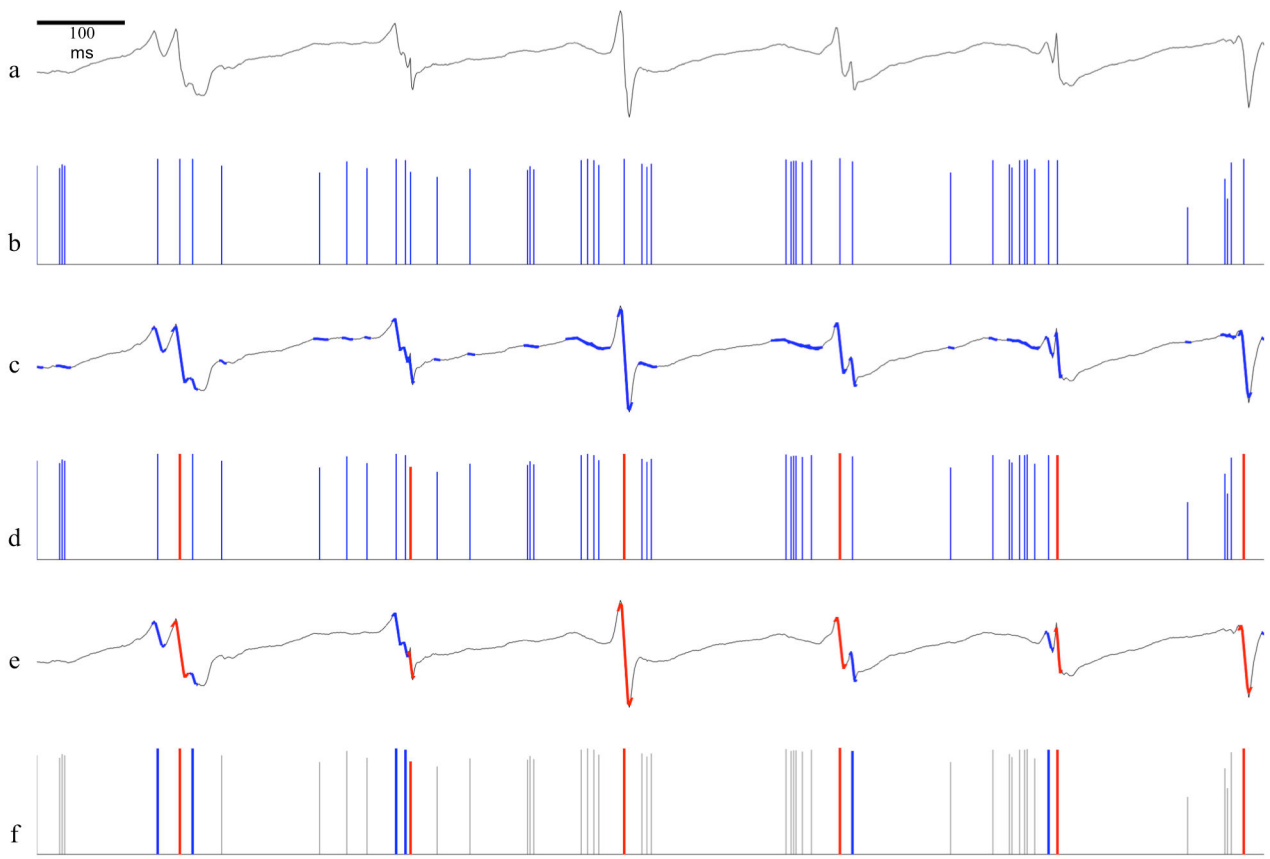

Figure 1. *Deflection detection procedure*. The pre-processed signal (a) is analyzed by a sensitive template-matching algorithm. The peaks in the correlogram are depicted in (b) and the corresponding template matches in (c). The intrinsic deflection assignment algorithm identifies the location of the intrinsic deflections (red) (d). Far-field deflections (blue) are determined as deflections that have a minimal amplitude of 10% of the median intrinsic deflection amplitude and a minimal slope of 10% of the median intrinsic deflection slope. The final result is depicted in (e) and the corresponding correlogram peak locations in (f).

electrograms these ventricular far-fields are usually relatively low in amplitude compared to the local atrial deflections, but nonetheless they can cause false positives when detecting deflections and constructing waves.

C. *Intrinsic deflection detection*

By interviewing several electrophysiologists, a single predefined deflection shape was constructed to detect all candidate atrial deflections in the electrograms. This template could vary in duration (5 - 50ms). At each time-point in an electrogram the maximum correlation was determined between the electrogram and all template durations. The local maxima in the resulting template correlogram were marked as candidate deflection positions, as shown in Fig. 1a, 1b and 1c. These candidate deflections can be either 1. true intrinsic (or local) deflections or 2. far-field deflections – fluctuations of the electrograms caused by activations remote from the electrode - or 3. deflections caused by external disturbances. To distinguish between the three types of deflections, we exploited the underlying distribution of the AF cycle length (AFCL). This distribution was estimated by iteratively increasing the minimally allowed deflection amplitude until the distribution of the remaining deflection intervals showed a clear peak. The position and shape of this peak in the interval distribution of deflections with higher amplitude reflect the interval distribution of the true intrinsic deflections. The distribution estimation procedure was automated by introducing a maximum deflection interval threshold (default value 250ms). The minimally allowed deflection amplitude was increased until a maximum percentage (default value 10%) of the remaining deflection intervals were larger than the maximum deflection interval threshold. A normal distribution with parameters $\theta_{\mathrm{CL}} = (\mu_{\mathrm{CL}}, \sigma_{\mathrm{CL}})$ was fitted on the resulting deflection intervals. The procedure is illustrated in Fig. 2.

Given the sequence of candidate deflections $\{c_n\}_{n\in\{1,2,\cdots,N\}}$ and the AFCL distribution estimate, a deflection type assignment problem is formulated, where the goal is to select a subsequence of intrinsic deflections $\{c_{n_r}\}_{r\in\{1,2,\cdots,k\},n_k\leq N}$ with maximum interval probability. Assuming a sequence of deflection intervals is i.i.d., the joint interval probability of a subsequence $\{c_{n_r}\}$ can be expressed as

$$P(\{c_{n_r}\}|\,\theta_{CL}) = \prod_{i=1}^{k-1} f(t_{r_{i+1}} - t_{r_i}|\,\theta_{CL}), \qquad (1)$$

where t_{r_i} is the central time of deflection c_i. The interval between the time t_{r_1} of the first deflection in a subsequence

and the beginning of the recording t_0 and the interval between the time t_{r_k} of last deflection in a subsequence and the end of the recording t_{end} has to be included in the joint probability of the subsequence to include the constraint that intrinsic deflections are to be found in all parts of the recording, forming a chain of deflections that are linked by probable deflection intervals.

$$P\left((t_0,\{c_{n_r}\},t_{end})|\,\theta_{CL}\right) = \tilde{f}(t_{r_1}-t_0|\,\theta_{CL})\cdot\left(\prod_{i=1}^{k-1} f(t_{r_{i+1}}-t_{r_i}|\,\theta_{CL})\right)\ldots \cdot \tilde{f}(t_{end}-t_{r_k}|\,\theta_{CL}), \quad (2)$$

where

$$\tilde{f}(t_j-t_i|\,\theta_{CL}) = \begin{cases} f(\mu_{CL}|\theta_{CL}) & \text{if } t_j-t_i \le \mu_{CL} \\ f(t_j-t_i|\theta_{CL}) & \text{if } t_j-t_i > \mu_{CL} \end{cases}. \quad (3)$$

A heuristic greedy algorithm finds a solution to the sequence selection problem by starting with the complete sequence of candidate deflections and trying to improve the joint deflection probability (2) by removing deflections, starting with deflection with low amplitude and slope, until the solution converges. This order of deflection deletion in this algorithm is based on the tendency of electrophysiologists to mark steep deflections with high amplitude as intrinsic deflections and flat deflections with low amplitude as far-field deflections. An example result of an intrinsic deflection assignment solution can be seen in Fig. 1d, 1e and 1f. The strength of this intrinsic deflection detection method is that it is able to adapt to substrate-specific deflection properties, such as amplitude, slope and interval distribution.

D. *Fibrillation wave construction*

The intrinsic deflection detection step determines the sequences of intrinsic deflections that are used to construct the fibrillation waves. The center of an intrinsic deflection is taken as the moment of local activation. Wave construction is divided into three phases. First, partial waves are created based on a minimum conduction velocity criterion (default value 20 cm/s) between two neighboring activations in the electrode grid. In experimental studies this threshold was identified as reasonable cut-off value for the occurrence of conduction block.[2] Activations that can be linked to two or more partial waves are not yet assigned. In the second phase statistical conduction properties of these partial waves are determined. The distribution of the wave conduction velocity is estimated by computing the conduction velocity in partial waves containing at least 9 activations. The local conduction velocity for each wave activation is determined by fitting a tangent plane onto the surface formed by the activation and the activations within the same wave at the directly surrounding electrodes. The conduction velocity is then computed as the reciprocal of the plane gradient vector length and the direction of conduction as the plane gradient angle. The resulting velocity distribution is approximated by a gamma distribution with parameters $\theta_{CV} = (\alpha_{CV}, \vartheta_{CV})$. Besides the velocity distribution also the distribution of the conduction deviation or *tortuosity* within a wave is determined by computing the mean conduction direction

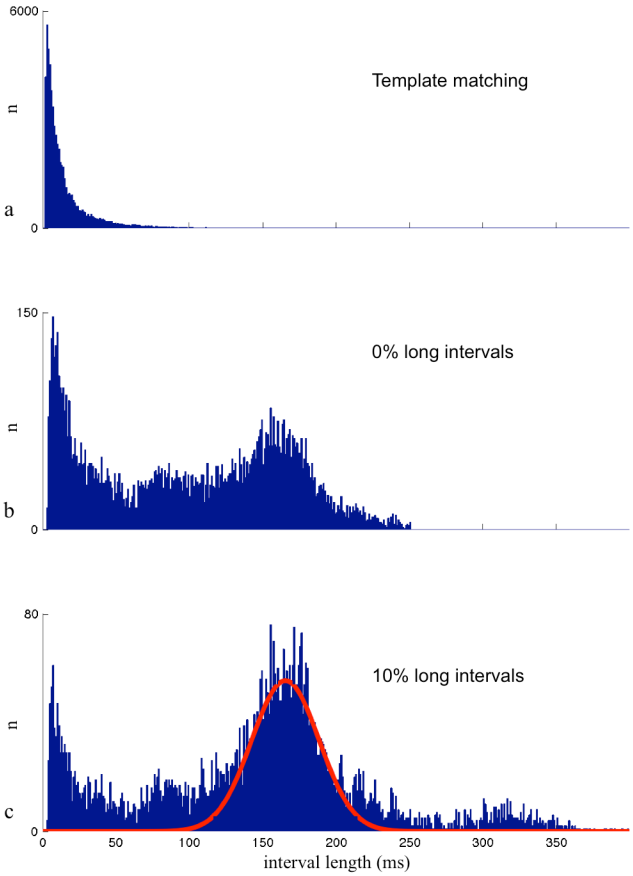

Figure 2. *Estimating the intrinsic deflection interval distribution*. A histogram of the intervals between the deflections found in the template matching procedure is shown in (a). Increasing the minimal amplitude of a deflection without causing long intervals, produces the histogram in (b). If a maximum of 10% long intervals are allowed, a clear peak appears, as can been seen in (c). A normal distribution is fitted onto this peak.

difference at each activation compared to the activations within the same wave at the directly surrounding electrodes. This tortuosity distribution is approximated by a normal distribution with parameters $\theta_{TO} = (\mu_{TO}, \sigma_{TO})$. The third phase consists of assigning the unassigned activations to adjacent waves based on a maximum local conduction velocity and conduction direction probability. Given an activation $a_{e,t}$ at electrode e at time t and a set of candidate waves W, this probability is defined as

$$P(CV = cv_{a,w}, TO = to_{a,w}) = P(cv_{a,w}|\theta_{CV})\cdot P(to_{a,w}|\theta_{TO}), \quad (4)$$

where $cv_{a,w}$ denotes the conduction velocity that results from adding activation $a_{e,t}$ to wave $w \in W$, and $to_{a,w}$ the mean conduction tortuosity.

E. *Validation*

The results of the novel automated deflection detection and wave map construction procedure were validated by comparing the location of intrinsic deflections to the location manually annotated deflections. Locations were considered equal if the manually annotated deflection was positioned within the descending part of the automatically detected

intrinsic deflection. Automatically computed wave maps were compared to manually constructed maps in terms of median wave conduction velocity, median AF cycle length, number of waves per AFCL, number of breakthrough waves (BT) per AFCL and average wave size.

III. Results and Discussion

The sensitivity of the intrinsic deflection detection algorithm compared to the manual intrinsic deflection annotation is 87±6.7% (mean±SD). The positive predictive value of the automated intrinsic deflection algorithm is 89±3.8%. Fig. 3 and Table 1 contain the comparison between the result of automated wave construction algorithm and the manually created waves. In general, the automated procedure produces very similar results to a manual annotation, most notably the wave conduction velocity and the AF cycle length. The number of waves per AFCL is only slightly overestimated, but the number of breakthrough waves per AFCL is roughly doubled by the automated procedure. An explanation for this phenomenon is that a manual editor tends to minimize the number of breakthroughs by searching for alternative activation pathways originating from the edge of the mapping array. A consequence of the larger number of waves detected in the automated procedure is that the average size of automatically created waves is smaller than the average size of manually created waves. Importantly, correlations are high, which effectively shows that the automated procedure is an adequately and valid substitute for the cumbersome manual annotation of atrial electrograms and manual atrial wave reconstruction.

TABLE 1. COMPARISON BETWEEN AUTOMATED AND MANUAL WAVE CONSTRUCTION. NUMBERS ARE REPORTED AS MEAN±SD. ALL CORRELATIONS ARE SIGNIFICANT ($P < 0.01$).

Category	Manual	Automated	r
Number of waves / AFCL	5.6±2.7	7.8±3.3	0.96
Number of BT / AFCL	1.8±1.2	3.7±2.0	0.94
Wave conduction velocity (cm/s)	65±12	66±13	0.97
AFCL (ms)	200±32	204±29	0.97
Wave size (number of electrodes)	53±29	36±18	0.96

IV. Conclusion

We developed and validated a novel algorithm for fast and automated spatiotemporal analysis of the substrate of atrial fibrillation. The algorithm identifies the key properties of the substrate with high accuracy. Potential applications of this technique are:

1. *Assessment of spatial and temporal variability of the AF substrate.* Automatic analysis of high-density maps during longer recordings will provide greater insight into the temporal variation in the behavior of the AF substrate and the recording duration required to assess AF complexity in a more reliable way.

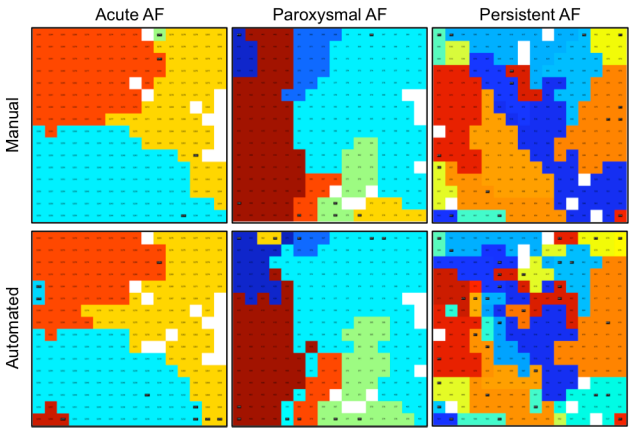

Figure 3. *Examples of manually edited wave reconstructions versus wave reconstructions computed by the automated procedure.* The maps show the wave reconstruction for a patient in acute AF, paroxysmal AF and persistent AF. The same wave shapes can be visually identified in both the manually edited maps as well as in the computed maps, although the automated procedure tends to create more and smaller waves. This does not however affect the ranking of AF complexity.

2. *Analysis of large amounts of fibrillation data in multicenter trials to establish a new classification of AF.* Using the automated method, the amount of AF fibrillation electrograms that can be feasibly processed and analyzed in a short amount of time will increase, enabling larger scale data studies required to establish a classification of AF.
3. *On-site AF substrate complexity assessment to tailor ablation therapy.* A (quasi) real-time implementation of the automated method can provide direct information on wave conduction patterns to guide the ablation process and can give immediate feedback to assess efficacy of an ablation lesion set.

References

[1] U. Schotten, S. Verheule, P. Kirchhof, and A. Goette, "Pathophysiological Mechanisms of Atrial Fibrillation: A Translational Appraisal," *Physiological Reviews*, vol. 91, no. 1, pp. 265–325, Jan. 2011.

[2] M. A. Allessie, N. M. S. de Groot, R. P. M. Houben, U. Schotten, E. Boersma, J. L. Smeets, and H. J. Crijns, "Electropathological Substrate of Long-Standing Persistent Atrial Fibrillation in Patients With Structural Heart Disease: Longitudinal Dissociation," *Circulation: Arrhythmia and Electrophysiology*, vol. 3, no. 6, pp. 606–615, Dec. 2010.

[3] P. Kirchhof, G. Y. H. Lip, I. C. Van Gelder, J. Bax, E. Hylek, S. Kaab, U. Schotten, et al., "Comprehensive risk reduction in patients with atrial fibrillation: emerging diagnostic and therapeutic options--a report from the 3rd Atrial Fibrillation Competence NETwork/European Heart Rhythm Association consensus conference.," *Europace*, vol. 14, no. 1, pp. 8–27, Jan. 2012.

[4] J. Pan and W. J. Tompkins, "A Real-Time QRS Detection Algorithm," *IEEE Trans. Biomed. Eng.*, vol. 32, no. 3, pp. 230–236, Mar. 1985.

[5] R. Alcaraz and J. J. Rieta, "Adaptive singular value cancelation of ventricular activity in single-lead atrial fibrillation electrocardiograms," *Physiol. Meas.*, vol. 29, no. 12, pp. 1351–1369, Oct. 2008.